Key Engineering Materials
ISSN: 1662-9795, Vol. 856, pp 135-142
doi:10.4028/www.scientific.net/KEM.856.135

Submitted: 2019-09-30
Revised: 2019-10-28
Accepted: 2020-01-31
Online: 2020-08-03

Effect of Fiber Laser Surface Modification on the Corrosion Behavior of 316L Stainless Steel

Rachapong Tangkwampian[1,a], Pornsak Srisungsitthisunti[2,b], Siriporn Daopiset[2,c] and Pruet Kowitwarangkul[1,d*]

[1]The Sirindhorn International Thai-German Graduate School of Engineering(TGGS), King Mongkut's University of Technology North Bangkok, Bangkok, 10800 Thailand

[2]Department of Production Engineering, Faculty of Engineering, King Mongkut's University of Technology North Bangkok, Bangkok, 10800 Thailand

[a]rchapong.t-mme2017@tggs.kmutnb.ac.th, [b]pornsak.s@eng.kmutnb.ac.th, [c]siriporn.d@eng.kmutnb.ac.th, [d]pruet.k@tggs.kmutnb.ac.th

Keywords: Corrosion, Fiber laser, Laser surface modification, Stainless steel, 316L

Abstract. This paper investigates the effect of fiber laser surface modification of AISI 316L austenitic stainless steel on corrosion behavior. In the experiments, the fiber laser with center wavelength of 1062 nm was employed with various laser parameters of beam velocity and laser frequency. The laser-treated has performed on the specimen surface in order to form the melted layer with an argon gas shielding. The electrochemical tested results showed that the laser-treated increases 40% pitting potential. Moreover, the results also exhibited corrosion potential shift to more positive potential. On the basis of the findings on the corrosion improvement, it can be concluded that the pitting potential of the material can be improved by a corrosion protective layer from the new laser-treated surface.

Introduction

Stainless steel is extensively used in various industries, for instance, oil and gas industries, automotive, marine, chemical and petrochemical industries. There are various types of stainless steel depending on its chemical contents, particularly FeCrNi which are the main elements in stainless steel. Nowadays, several problems of the stainless steel have been reported, for instance, intergranular corrosion in welded materials [1] and atmospheric corrosion in Thailand environment [2]. In the past two decades, there are several techniques to improve the stainless steel corrosion by chemical treatment [3-4], surface bioactive coating by sol–gel technique [5], and laser surface treatment by several types of laser in the market [6-10]. The study of S. Kkalainathan et al. showed that the 316L surface stress was improved by laser shock peening from 12 MPa to 273 MPa and corrosion potential was also improved [6]. In 2010, J.Z.Lu et al. published the study of grain refinement mechanism by using multiple laser shock process on ANIS 304 steel. It was found that the effects of multiple laser shock peening (LSP) impacts on microstructure cause refined grain boundaries [7]. In addition to LSP process, the excimer laser surface treatment can also improve the pitting corrosion resistance of 316LS stainless steel [9].

The laser techniques are beneficial for the improvement of surface materials especially stainless steel. Among several research studies on laser surface treatment, fiber laser is one of the laser types in the present market, especially for the decoration industry. E.H.Amara has studied fiber laser color marking on 316L steel. The fiber laser power from 2-10 w was employed in his research. The results showed that the main effect of the laser treatment is an energy supply. Another interesting result was that the chemical composition in the oxide film layer has changed [11]. However, there has been a small number of research studies regarding the corrosion for decorated surface by fiber laser.

Therefore, in this current study, the fiber laser with the center wavelength of 1062 nm (±3 nm) was employed for laser surface modification of AISI 316L stainless steel. The laser treating on the material surface was performed in order to improve the corrosion of the material. Microstructure

and surface morphology was examined by the comparing various laser parameters. Electrochemical test was applied to study the corrosion behavior by using cyclic potentiodynamic polarization technique.

Experimental

Material and specimen preparation The austenitic stainless AISI 316L specimens with chemical composition given in Table 1 were selected to perform the surface modification by fiber laser in this experiment. The as-received material was in the form of stainless steel plate with 2 mm. of thickness.

Table 1 Chemical composition of AISI 316L stainless steel [wt.%].

Fe	Cr	Ni	Mo	Mn	C	P	S	Si
Bal	16.65	10.35	2.02	1.39	0.026	0.072	0.023	0.28

Fiber laser modification was performed on a rectangular AISI 316L stainless steel. The specimens were fiber cut to the desired shape of 25 mm × 40 mm × 2 mm. as shown in Fig. 1(c). Before performing laser surface modification, the specimens were polished up to 360 grit of SiC abrasive paper and cleaned by an ultrasonic washing bath in an acetone solution for 15 minutes.

Laser surface modification This experiment was carried out by using 50 W fiber laser (JenlasfiberNS50). Fig. 1(b) represents the basic mechanism for this experiment. The laser was operated at 1062 nm (±3 nm) of center wavelength and 0.7 mJ of maximum pulse energy. The laser beam was generated in a pulsed operation mode moving along the laser moving path direction at different velocity of 0.35 mm/s and 0.7 mm/s, and different laser repetition frequency of 10 kHz and 20 kHz. The laser power, hatch distance, and infill line velocity were set at 50 W, 25 µm, and 0.03 mm/s, respectively. The laser spot shape occured from pulsed beam was in several overlapping circles along the laser moving path. Fiber laser modification conditions used in this study is shown in Table 2.

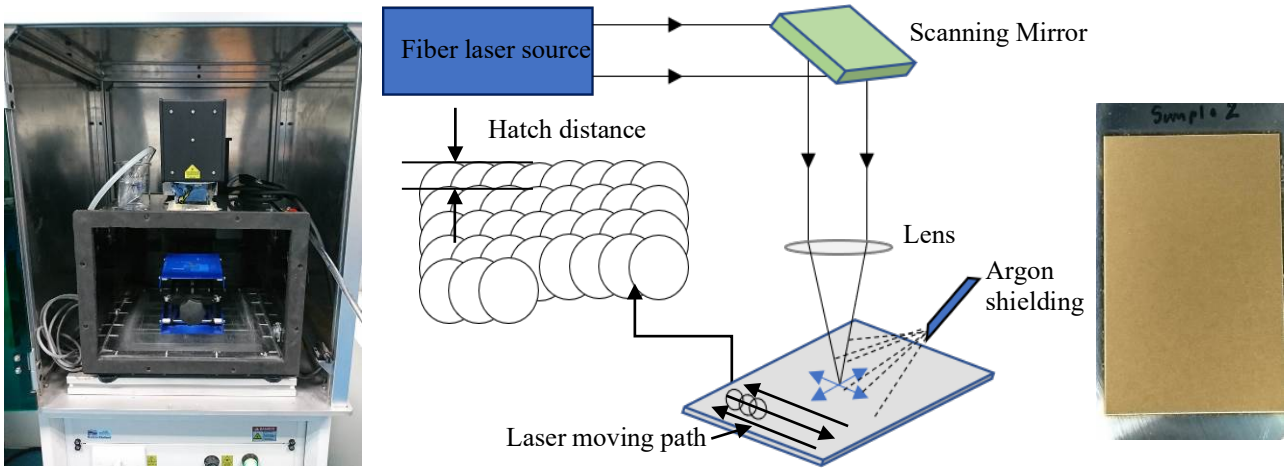

(a) (b) (c)

Fig. 1 (a) JenlasfiberNS50 machine, (b) Schematic of fiber laser experiment set-up, (c) Example of the test specimen.

The laser beam tracks were in different overlapping percentage due to the laser parameters. Fiber laser modification was operated under an argon shielding gas at a flow rate of 15 l/min in order to avoid oxygen contamination.

Table 2 Research experimental parameters.

Specimen	Beam velocity [mm/s]	Repetition frequency [kHz]
LM-1	0.35	10
LM-2	0.7	10
LM-3	0.35	20
LM-4	0.7	20
Base material (BM)	-	-

Microstructural analysis The surface morphology of the test specimens was performed by taking the perpendicular cross-section to the laser hatch distance using a fiber cutting machine to get the desired shape. The surface of all specimens were prepared by grinding with 120-2000 grit of SiC abrasive paper, then polishing with the aluminum oxide paste. 10% of oxalic acid was used for the electrochemically etching on the polished surface. In addition, 7 volts of potential was applied during the process for 45 seconds.

Corrosion studies After the fiber laser modification process, the samples were cleaned by an ultrasonic washing bath with an acetone for 10 minutes to remove dust, dirt on the surface before the corrosion test. Corrosion behaviors of the specimens were evaluated based on electrochemical technique.

Laser surface modification and BM samples were tested in 3.5% NaCl solution at room temperature by means of electrochemical methods obtaining free corrosion potential–time and polarization curves. The solution was prepared with distilled water by weighing 70 grams of sodium chloride (35 grams per 1000 milliliters of water). The prepared sodium chloride was poured into distilled water 2000 milliliters, then stirred the mixed solution until sodium chloride completely dissolved.

Fig. 2 (a) Self-invented corrosion cell, (b) Biologic science instruments VMP2 multichannel potentiostat.

The corrosion tests were performed using a self-invented corrosion cell based on conventional three-electrode corrosion cell with SCE calomel (saturated KCL) as a reference electrode. In the experiment, platinum was used as a counter electrode as shown in Fig. 2(a). The sample surface area exposed to the electrolyte was 0.28 cm^2. In this study, the specimens were investigated with a

Biologic science instruments VMP2 multichannel potentiostat via the EC-Lab program with cyclic potentiodynamic polarization technique to study the corrosion behavior as illustrated in Fig. 2(b). To begin the corrosion test, firstly, open circuit potentials of the samples were measured for 30 minutes. Then, the cyclic potentiodynamic technique was performed at a potential scan rate of 0.8 mV/s.

Results and Discussion

Characterization of laser surface modification

Laser surface observations Base on the results of the current study, it can be summarized that after laser surface modification processes with argon gas shielding was performed, the surface morphology between base material (BM) and laser treated-surface modification exhibited extremely different surface. Various beam velocities and the laser pulse frequency ranges which generate overlapping lines have effects on laser spot's concentrations. The results showed similarity between the overlapping distance of LM-1 and LM-4. Fig. 3(b) and Fig. 3(e) shows that each specimen presents overlapping percentage at approximately 60%. Refer to W. Pacquentin, the study showed that the specimen subjected to laser treatment with overlapping laser spots for AISI 304L austenitic stainless steel exhibited high chromium content in the oxide layer. The study pointed out that the sample with 70% and 90% overlapping rate have attributed to the formation of a homogeneous oxide layer with high chromium enrichment 47 wt.% and 31 wt.%, respectively[11,12]. Therefore, the overlapping laser spot intensity significantly affects the enrichment of chromium content in the oxide layer that the chromium content plays an important role in corrosion resistance of the austenitic stainless steel.

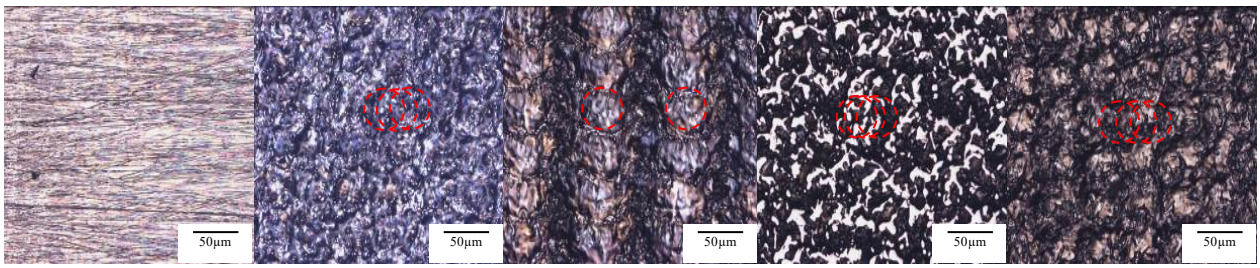

Fig.3 Effect of the laser parameters on the specimens' surface (a) BM;No laser (b) LM-1;0.35mm/s, 10 kHz. (c) LM-2;0.7 mm/s, 10 kHz. (d) LM-3;0.35 mm/s, 20 kHz. (e) LM-4;0.7 mm/s, 20 kHz.

The investigated results showed the specimens with microporous and irregular surfaces. This is due to the energy supply which was re-melted and also generated heat on the specimens' surface [13]. The concentration of the laser spots was influenced by the beam velocity. The increase in the laser velocity affects less laser spot repetition; on the contrary, the decrease in the laser velocity affects more laser spot repetition and more surface penetration area. The different laser spot concentration is shown in Fig. 3(b)- Fig. 3(e).

Microstructural analysis The specimen cross-section showed a surface morphology of the nearly melted zone from the laser surface modification by the solidification process in the air environment for all specimens with 4 – 40 µm depth. To analyze the microstructure of the laser-treated surface, the deformation results was observed near the laser-treated surface as shown in Fig.4. The grain refinement can be seen under the laser-treated surface approximately 10 µm depth. The important key of the grain refinement was a strain rate, the key phenomenon which contributed to the ultra-high strain rate was an ultrashort fiber laser pulse during the laser surface modification. The grain size can be significantly reduced when power density that is performed on the surface increase [6]. The results of the grain refinement can be obviously seen on the top surface of specimen as shown in the Fig.4(b)-(e). Since the highest frequency and the lowest beam velocity result in high power density on the specimens' surface; therefore, it causes a thermal contraction with high strain rate, high density dislocation and plastic deformation to induce refined grains [7].

Apart from the high strain rate, refer to J.Z.Lu et al.[8], during laser surface modification can be refined the grain size. The study pointed out that the grain refinement in fcc materials can also be caused by intersectional microstructure aligned in multiple directions due to the mechanical twins intersection.

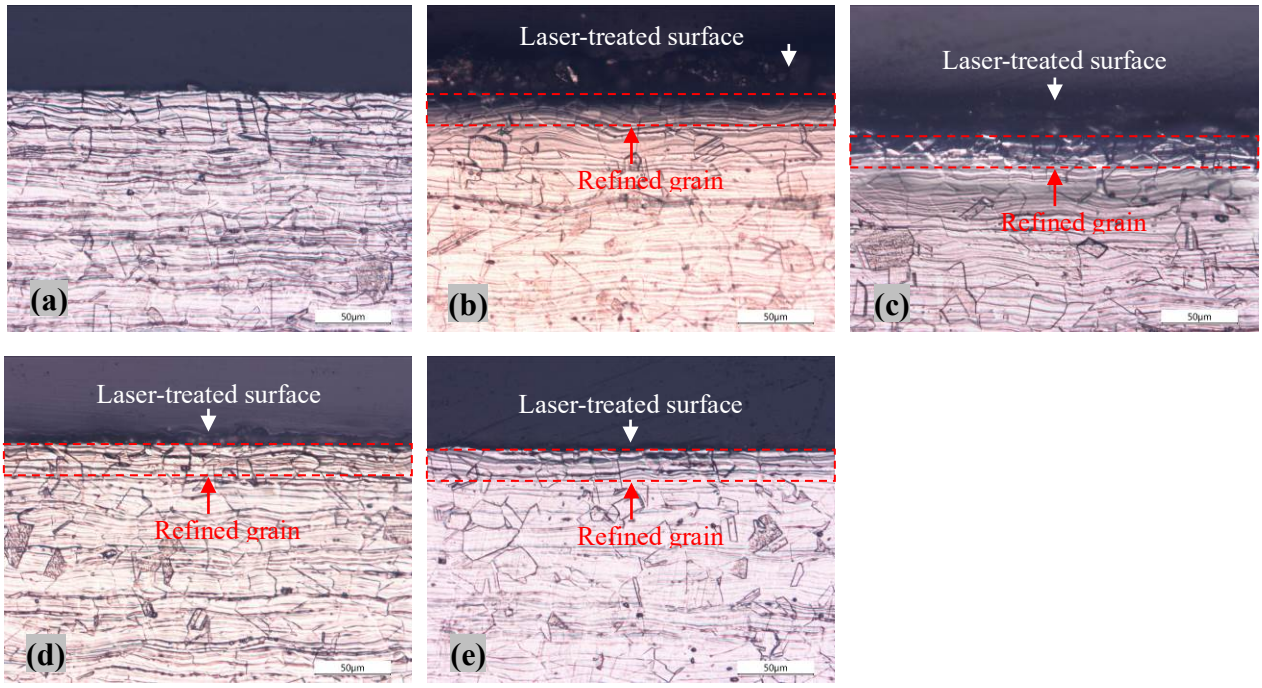

Fig.4 Microstructure of the LM surface, electrochemical etched with 10% oxalic acid (a) BM;No laser (b) 0.35 mm/s, 10 kHz (c) 0.7 mm/s, 10 kHz (d) 0.35 mm/s, 20 kHz (e) 0.7 mm/s, 20 kHz.

Corrosion The potential versus time curve in Fig. 5(a) represents the open circuit potential of the material which anodic and cathodic rates were in the equilibrium. The resulted from the open circuit curves are: -360 mV for BM and LM-3 > LM-1 > (LM-2, LM-4) were -260 mV, -300 mV, -320 mV, respectively. The information gathered from the open circuit curves can be summarized that the starting potential for all specimens rapidly dropped to more negative potential values for 400 seconds, then the OCP would decrease slightly and became more stable until 1800 seconds, for all laser-treated specimens remained around -300 mV while BM specimens remained around -360 mV. However, after OCP potential dropped, the BM specimen slightly changes compared with LM specimens. Nonetheless the OCP values of most of LM specimens shifted to more negative potential values compared to that of the BM specimens. The subsistence of the laser surface-melted layer was the cause of shifted OCP potential values to more negative potential.

Cyclic potentiodynamic polarization curves are given in Fig. 5(b). The potential versus current density curve represented a corrosion potential (E_{corr}), corrosion current density (I_{corr}) and pitting potential (E_{pitt}), all information has been determined by theoretical tafel plot form the polarization curve [15]. All the laser surface modification specimens when it has been applied potential to the passive stage, the corrosion potential results exhibit the shifted to more corrosion potential (less negative values) than that of un-treated specimen (BM).

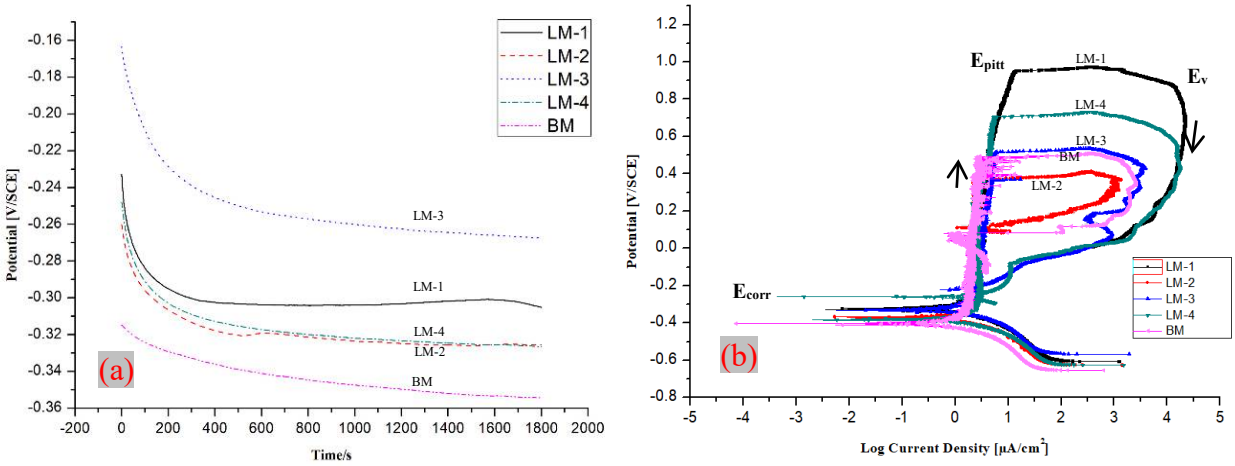

Fig. 5 Representation of corrosion graph results (a) Comparison of open circuit potential vs time, (b) Potentiodynamic polarization curves.

For the passive region, it can be summarized that two specimens out of four, LM-1 and LM-4 exhibited the higher passive film range until corrosion took place at a breakdown potential (E_{pitt}) by the specimen LM-1 (0.35 mm/s of beam velocity, 10kHz) experienced the highest pitting potential at 953 mV. This means that the protective film of the laser modification surface has the ability to persist the corrosion to take place this is due to the chromium enrichment in the oxide film layer. The corrosion resistance of stainless steel is excellent this is due to the passive chromium oxide film which forms on the stainless steel surface. Generally, the stainless steels which contain high chromium content play a key role in high corrosion resistance [16]. The surface finishing process can enrich the chromium content in the oxide film, the surface finished that can enriched chromium will effectively prevent the corrosion [17,18]. Refer to Kwok et al. [19], the study evidenced that the pitting resistance increase with the decrease in grain size.

Table 3 The mean of corrosion tested results for all specimens.

Specimen	**E_{pitt} [mV]**	**I_{corr} [μA/cm^2]**	**E_{corr} [mV]**	**ΔE [mV]**
LM-1	953	0.72	-325	1299
LM-2	373	0.74	-373	784
LM-3	517	0.70	-329	865
LM-4	706	0.74	-332	1108
Base material [BM]	542	0.46	-401	1054

The current density for all specimens in Table 3 shows the shift of a higher value from 0.4 to 0.7 μA/cm^2 due to the effect of the irregular surface. Due to the irregular of the laser surface, actual corrosion testing area could not measure the exact values. This will affect the corrosion current density per unit area and exhibit the fluctuating value.

After breakdown potential, this state showed the re-passivation film ability. All laser specimens had the ability to re-passive the protective film again (see details in Fig. 5(b)). Furthermore, the area of a hysteresis loop size after the breakdown potential (E_{pitt}) was the area after the forward curve started to reverse (E_v) toward the negative potentials due to the formation of the passive film layer on the specimens' surface until it crossed the forward polarization curve. The bigger size of the hysteresis loop implies more disruptive of the passive making it difficult to restore the passive film after localized corrosion (crevice and pitting corrosion) took place [20]; nevertheless, if the specimens tested under the same conditions (testing solution, temperature), the susceptibility of crevice corrosion can be also determined by comparison of the loop sizes [21].

From the cyclic potentiodynamic polarization curves shown in Fig. 5(b), although passive film can be restored, the results showed that the laser surface modification specimens exhibited more

susceptible to the localized corrosion than that of BM specimen due to the high hysteresis loop. The two difference parameters form the cyclic potentiodynamic polarization, the corrosion potential (E_{corr}) and vortex potential (E_v) can be used to determine the stability of the protective oxide film layer (ΔE**)**. The parameters $\Delta E = E_v - E_{corr}$, that E_{corr} is the corrosion potential in the forward scan and E_v is the potential value which was the point of scan reversal. The greater amount of ΔE represented more protective oxide layers [22]. In Table 3, the ΔE results showed that the specimens LM-1 and LM-4 exhibited the greater protective oxide layer than the base material specimen caused by the existence of the laser surface.

S**ummary**

Laser surface modification by fiber laser on AISI 316L stainless steel evidenced that the laser parameters affected directly to the surface morphology and grain refinements due to the high strain rate resulting from an increase of power density on the surface. The change of laser frequency and beam velocity have a significant influence on the laser overlapping percentage. In this study, the experiment showed that 60% overlapping exhibited the greater pitting potential than BM specimen from 542 mV to 953 mV due to the subsistence of laser modification surfacen, as well as the chromium enrichment in the protective oxide film layer. The specimen LM-1 with 0.35 beam velocity and 10 kHz of frequency exhibited the highest corrosion potential from -401.992 to -325.239 mV. On the other hand, the specimen LM-2 with 0.7 beam velocity and 10 kHz exhibited worse results than that of the base material. However, the laser specimens can re-passive the film itself, but there are more susceptible to localized corrosion than the base material, AISI 316L. This is due to the high area of the hysteresis loops.

Future studies will focus on the laser-treated surface layer characterization by the Energy Dispersive X-ray Spectroscopy (EDX) technique to study the change of elemental composition after the fiber laser surface modification.

Acknowledgements

This research was funded by King Mongkut's University of Technology North Bangkok. Contract no. KMUTNB-61-GOV-01-12. Lastly, the author is thankful to the Thai-French Innovation Institute, Corrosion Inhibitor Testing Laboratory and Miss.Paweena Treewiriyakitja for supporting the corrosion basic study as well as an experimental setup.

References

[1] C. Garcia, M. P. De Tiedra, Y. Blanco, O. Martin, F. Martin, Intergranular corrosion of welded joints of austenitic stainless steels studied by using an electrochemical minicell, Corros. Sci. 50(8) (2008) 2390-2397.

[2] D. Siriporn, K. Noparat, C. Somsiri, Atmospheric Corrosion of Stainless Steels in Thailand, King Mongkut's University of Technology North Bangkok International Journal of Applied Science and Technology 5, 1 (2012) 63-69.

[3] Y. C Lu, M. B. Ives. Chemical treatment with cerium to improve the crevice corrosion resistance of austenitic stainless steels. Corros. Sci. 37(1) (1995) 145-155.

[4] N. Le Bozec, C. Compere, M. L'Her, A. Laouenan, D. Costa, P. Marcus, Influence of stainless steel surface treatment on the oxygen reduction reaction in seawater, Corros. Sci. 43(4) (2001) 765-786.

[5] C. Garcia, S. Cere, D. Alicia, Bioactive coatings prepared by sol–gel on stainless steel 316L, J. Non-Cryst. 348 (2004) 218-224.

[6] S. Kalainathan, S. Sathyajith, S. Swaroop, Effect of laser shot peening without coating on the surface properties and corrosion behavior of 316L steel, Opt. Laser. Eng. 50(12) (2012) 1740-1745.

[7] C. Carboni, P. Peyre, G. Beranger, C. Lemaitre, Influence of high power diode laser surface melting on the pitting corrosion resistance of type 316L stainless steel, J. Mater. Sci. 37(17) (2002) 3715-3723.

[8] J. Z. Lu, K. Y. Luo, Y. K. Zhang, G. F. Sun, Y. Y. Gu, J. Z. Zhou, X. D. Ren et al, Grain refinement mechanism of multiple laser shock processing impacts on ANSI 304 stainless steel, Acta Materialia 58, 16 (2010) 5354-5362.

[9] T. M. Yue, J. K. Yu, H. C. Man, The effect of excimer laser surface treatment on pitting corrosion resistance of 316LS stainless steel, Surf. Coat. Tech. 137(1) (2001) 65-71.

[10] P. Peyre, X. Scherpereel, L. Berthe, C. Carboni, R. Fabbro, G. Béranger, C. Lemaitre, Surface modifications induced in 316L steel by laser peening and shot-peening. Influence on pitting corrosion resistance, Mater. Sci. Eng: A 280 (2) (2000) 294-302.

[11] W. Pacquentin, N. Caron, R. Oltra., Effect of microstructure and chemical composition on localized corrosion resistance of a AISI 304L stainless steel after nanopulsed-laser surface melting, Appl. Surf. Sci. 356 (2015) 561-573.

[12] W. Pacquentin, N. Caron, R. Oltra., Nanosecond laser surface modification of AISI 304L stainless steel: Influence the beam overlap on pitting corrosion resistance, Appl. Surf. Sci. 288 (2014) 34-39.

[13] E. H. Amara, F. Haïd, A. Noukaz, Experimental investigations on fiber laser color marking of steels, Appl. Surf. Sci. 351 (2015) 1-12.

[14] L. Y. Qin, X. D. Wang, F. L. Song, Y. Jao, S. H. Luo, Effect of Residual Stress and Microstructures on 316 Stainless Steel Treated by LSP, In Materials Science Forum. 898 (2017) 1261-1265.

[15] J. A. Denny, Principles and Prevention of Corrosion, 2nd ed., Prentice Hall., 1995

[16] K. Asami, K. Hashimoto, Importance of initial surface film in the degradation of stainless steels by atmospheric exposure, Corros. Sci. 45(10) (2003) 2263-2283.

[17] T. Hong, T. Ogushi, M. Nagumo, The effect of chromium enrichment in the film formed by surface treatments on the corrosion resistance of type 430 stainless steel, Corros. Sci. 38(6) (1996) 881-888.

[18] P. Lacombe, B. Baroux, G. Beranger, Stainless Steels, Les Editions de Physique Les Ulis, France, 1993

[19] C. T Kwok, F. T. Cheng, H. C. Man, W. H. Ding, Corrosion characteristics of nanostructured layer on 316L stainless steel fabricated by cavitation-annealing, Mater. 60(19) (2006) 2419-2422.

[20] S. Esmailzadeh, M. Aliofkhazraei, H. Sarlak, Interpretation of Cyclic Potentiodynamic Polarization Test Results for Study of Corrosion Behavior of Metals: A Review, Prot. Met. Phys. Chem. 54(5) (2018) 976-989.

[21] K. R. Trethewey, J. Chamberlain, Corrosion for Science and Engineering, Longman, Harlow, 1995

[22] N. Cotolan, A. Pop, D. Marconi, O. Ponta, L. M. Muresan, Corrosion behavior of TiO2-coated Ti–6Al–7Nb surfaces obtained by anodic oxidation in sulfuric or acetic acid, Mater. Corros. 66(7) (2015) 635-642.